Computational Investigations into the Potential Use of Poly(benzyl phenyl ether) Dendrimers as Supports for Organometallic Catalysts

Kevin J. Naidoo,* Samantha J. Hughes, and John R. Moss

Department of Chemistry, University of Cape Town, Rondebosch 7701, South Africa

Received July 17, 1998; Revised Manuscript Received October 20, 1998

ABSTRACT: We studied the structure and conformation of organic and organochromium poly(benzyl-phenyl ether) dendrimers (PBPE dendrimers) via atomistic molecular dynamics computer simulations. The results of our computational investigations show that the metal carbonyl centers are available to participate in chemical reactions. When the results of a course-grain computer simulation study by Murat and Grest[1] were used, this conclusion was valid for all solvent conditions. The terminal groups of both the organic and organochromium dendrimers smaller than generation 3 ($g_{max} \leq 3$) undergo significant backfolding and are capable of penetrating the central (core) region. However in the organochromium case, for $g_{max} > 3$ the terminal ((benzyl)tricarbonylchromium(0)) groups do not penetrate the core region to the same extent as do the terminal (benzyl) groups in the organic dendrimers of similar generation. This is mainly due to molecular crowding. By calculating the fractal dimensions we are able to determine that both dendrimer types are compact structures. However, despite their compact nature the terminal groups of the later organochromium polymers are solvent accessible and hence spatially available to act as catalysts in chemical reactions.

1. Introduction

It has been two decades since the idea of "cascade synthesis" was first introduced; this led to work on starburst dendrimers culminating in the synthesis of the first dendritic polymers by Tomalia and co-workers.[2] Since then many papers have described the synthesis and properties of a variety of dendrimers. The reason for the great interest in this unique class of polymer goes beyond its novel architecture consisting of short chains built around an initiator core. These macromolecules have the promise of applications which include acting as drug delivery systems[3,4] and as super catalysts.[5] It is the application as super catalyst that inspired the synthesis of one of the first organometallic dendrimers in our laboratories a few years ago.[6] Since then many metals have been incorporated into organic dendrimer structures, including iron, platinum, tungsten, gold, rhodium, palladium, copper, ruthenium, nickel, chromium, and osmium.[7,8] A review of organometallic and related metal-containing dendrimers synthesized to date is published elsewhere.[9]

The application of organometallic dendrimers as catalyst supports could bridge the divide between homogeneous and heterogeneous catalysis. Homogeneously catalyzed reactions are typically far faster and more selective than their heterogeneous counterparts; however, it is difficult to separate the catalyst from the product mixture. Dendrimers could provide a solution to this problem. The terminal groups and the organic skeleton are soluble in common organic solvents; consequently, catalytically active metals complexed at the periphery are able to catalyze reactions homogeneously.

We are presently investigating Frechet type[10] poly(benzylphenyl ether) dendrimers (PBPE dendrimers) via computer simulations. In addition we are investigating, via convergent synthesis, the functionalization of the peripheral aromatic rings as (arene)tricarbonylchromium(0) complexes. Throughout this paper we will refer to these macromolecules as organochromium dendrimers. These dendrimers consist of four distinct chemical units: the "core" molecule, 1,1,1-tris(4′-hydroxyphenyl)-ethane (shown in Figure 1(a)); the main repeat-unit, 3,5-dihydroxybenzyl alcohol (shown in Figure 1(b); the surface functionalities, a benzyl group in the organic dendrimers; and a (benzyl)tricarbonylchromium(0) complex in the organometallic dendrimers (shown in Figure 1(c) and (d), respectively).

In the synthesis of a PBPE dendrimer (Figure 2(a)), two surface groups react with 3,5-dihydroxybenzyl alcohol to form a first generation wedge. This wedge contains two ether linkages, one between each surface group and what was formerly 3,5-dihydroxybenzyl alcohol. This benzyl phenyl ether linkage is found throughout the dendrimer, not only in connecting surface groups to interior monomers, but also where monomers are linked to each other and to the core. The conformation of the ether link is extremely important, and can be completely defined by three torsion angles: Φ, Ψ, and Ω, as shown in Figure 2(b). We have therefore investigated the conformational space of the ether linkage and report these results in section 4.1.

In comparison with the wealth of literature on the synthesis and properties of dendrimers, the number of reports providing structural information is very limited. These compounds are difficult to crystallize, hence only crystal structures of small dendritic wedges have appeared in the literature.[11] A novel application of rotational-echo double-resonance NMR (REDOR) on fifth generation Frechet type dendrimers has been used to probe the solid-state structure of PBPE organic dendrimers.[12] In the REDOR experiments dipolar couplings between ^{13}C atoms located near the chain ends and an ^{19}F label placed at the core of generation 1−5 benzyl ether dendrimers were used to investigate their shape, size, and intermolecular packing. Although the solid-state structure of dendritic macromolecules is of great importance, experiments investigating dendritic polyethers in solution are of specific interest to the study of

* To whom correspondence should be addressed.

10.1021/ma981135g CCC: $18.00
Published on Web 01/08/1999

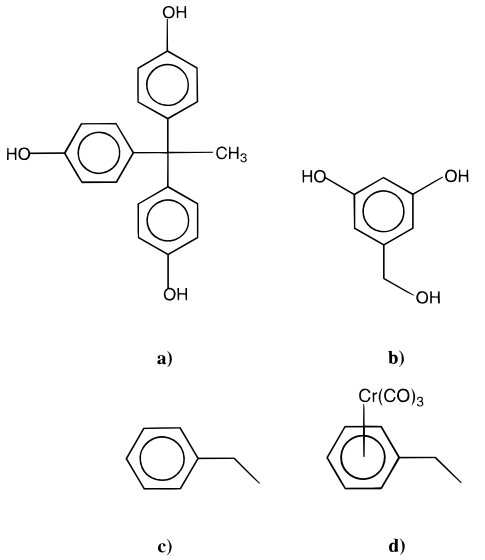

Figure 1. (a) The PBPE dendrimer core. (b) 3,5-Dihydroxybenzyl alcohol. (c) The benzyl surface group for the organic dendrimer. (d) The surface complex (benzyl) tricarbonylchromium(0) for the organochromium dendrimer.

dendrimers as catalyst supports. One such experiment was performed by Hawker et al.[13] where a solvatochromic molecule was inserted into the "core" of a polyether dendrimer and the UV absorption maximum was monitored for generations 0−6 in a variety of solvents. In addition, the solution structure of a series of iron−sulfur core dendrimers of the form $(n\text{Bu}_4\text{N})_2[\text{Fe}_4\text{S}_4(S\text{-Dend})_4)]$ was experimentally investigated.[14] The NMR experiment relies on the paramagnetic core $\text{Fe}_4\text{S}_4(S-R)_4^{2-}$ to investigate the proximity of nuclei in the dendrimers 1−3 to the core. These dendrimers are topologically very different from the PBPE dendrimers we report here.

The results of experimental attempts at elucidating the structure of these complex macromolecules are limited to the specific cases under investigation because the solution structure of dendrimers varies on the basis of inherent topology of the macromolecules. The nature of the branch points, flexibility of spacers, and as we will show, even the chemical structure of the terminal groups affect the conformation. However, many computational efforts are focused on general structural features of dendrimers. Computational and theoretical techniques have been used to investigate dendritic conformation. The first attempt to analyze dendrimer structure was via a mean-field approach.[15] The authors, de Gennes and Hervet, employed a self-consistent field on model dendrimers consisting of branch points connected by flexible linear portions (spacers). On the basis of the assumption that the spacers are strongly elongated and that the spacers of each generation lie in a concentric shell of their own, oriented away from the core, they investigated the "limiting generation number" beyond which perfect starburst growth is impossible. The main conclusions drawn from this theoretical analysis were that a limiting generation number does exist, and that it is an increasing function of spacer length. In addition, the densities of the dendrimers are at a minimum near the core, and increase to a maximum at the surface,[15] with the result that the macromolecule should be flexible in the inner shell and rigid at the periphery. This conclusion results in a prediction that the branch ends lie exclusively on the surface of the molecule.[15]

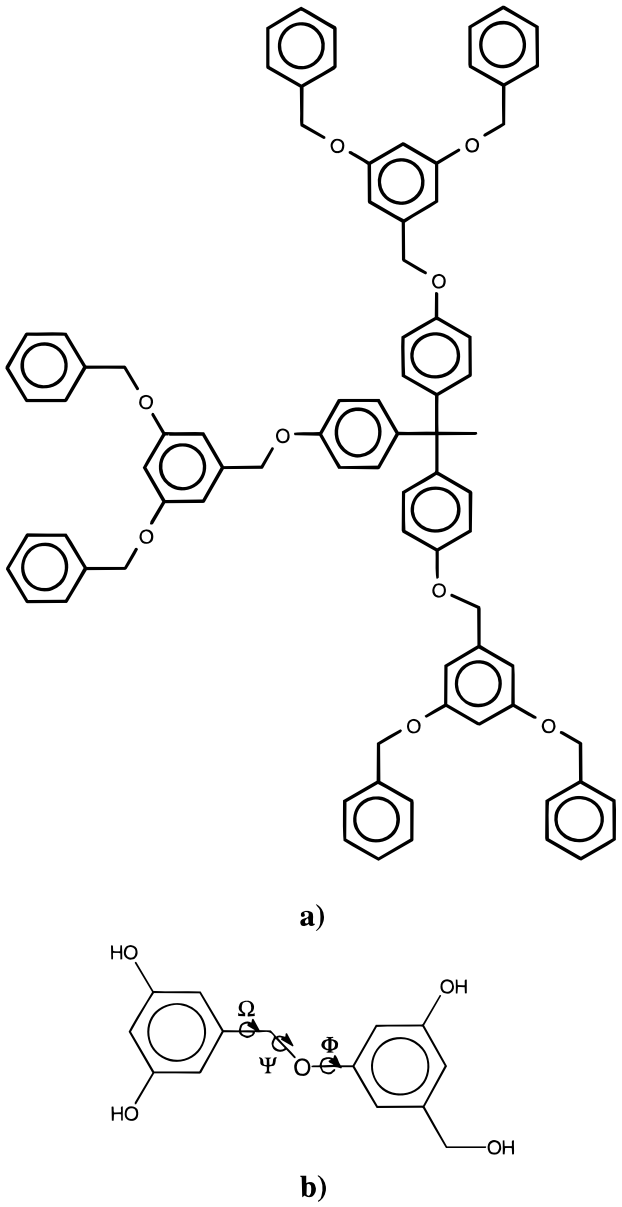

Figure 2. (a) First generation organic dendrimer. (b) The "dimer" used to derive the starting dendrimer structures for the molecular dynamics simulations.

De Genne's mean-field analysis provided a basis for comparison for all subsequent dendrimer simulation studies. These computer simulations were performed on two length scales: monomer-level (coarse grained) calculations, which do not take into account atomic detail, and atomistic simulations, which include molecular detail in the simulation model.

1.1. Monomer-Level Simulations of Dendrimers. Very few examples of atomistic calculations on dendrimers exist in the literature, and most of these focus on the polyamidoamine (PAMAM) dendrimer system.[2,16,17] There have, however, been several monomer-level studies based on a PAMAM branching functionality and spacer lengths.[18−20] The PAMAM and PBPE dendrimers have the same branch point multiplicity (number of branches at each branching point, $N_b = 2$) and initiator-core multiplicity (number of wedges originating from the core, $N_c = 3$). This would make these dendrimers topologically far more similar to each other than to other dendrimers with different branch point

and initiator-core multiplicities. The results of these calculations could be transferable to PBPE dendrimers. Because of the topological similarity of the two systems, we briefly discuss results from the coarse-grained simulations which are directly relevant to the PBPE dendrimers.

Several groups have simulated model dendrimers using Monte Carlo methods or MD simulations[1,18−20] and compared the results with the predictions of de Gennes and Hervet. In most of the studies, the dendrimers were modeled as strings of beads, with trifunctional branch points, and flexible spacers. In some cases, the functionality of the branch points and the spacer lengths were chosen specifically to closely match PAMAM dendrimers.[18−20] This might provide a point of departure from the mean-field results, because PAMAM spacers are fairly short, whereas the de Gennes−Hervet model was based on long spacer lengths.

Most of the simulation studies show that the dendrimer density distribution is highest at the center, and decreases outward toward the surface of the molecule.[18−20] This is in complete disagreement with the de Gennes−Hervet model, where a maximum at the periphery is predicted.[15] For some dendrimers, notably the higher generations, an interesting phenomenon is observed. When moving outward from the center, the density decreases rapidly to a local minimum, then increases again before continuing the general decline.[20,21] One of these studies correlated internal voids close to the center to this local minimum in density.[21]

In conjunction with the density distribution studies were efforts to locate the terminal groups of the dendrimers. Spatial location of these monomers is necessary for structural analysis, but is of particular importance if the dendrimer is intended as a catalyst support. The catalytically active metals could be bound on the outer generation of the dendrimer, but not necessarily physically present at the periphery of the molecule. If chain folding occurs to a large or even moderate extent, then the active sites might be buried deep within the dendrimer and would thus not be accessible for catalysis.

1.2. Atomistic Simulations of Dendrimers. Atomic-level calculations provide more detail than the coarse-grained models, and properties specific to the chemical system under investigation could be more easily probed. In addition, certain properties are exclusively available via atomistic techniques. One such property is the solvent accessible surface (SAS) of dendrimer terminal groups that are directly relevant to our interest in a catalysis application. Moreover, all of the properties examined at the monomer-level simulations can also be calculated from atomic-level calculations, including relaxation times, dendron segregation, and density distributions. Despite these advantages a major drawback of the technique is the limited system size that can be investigated. This becomes especially significant when solvents are explicitly included in the model.

Recently there have been atomistic simulations of PBPE dendrimers.[22] However, there has not been any comprehensive structural data on organometallic dendrimers published to date, but rather very limited molecular mechanics-based calculations on metalloporphyrin-dendrimers[23,24] and metallodendrimers.[25] Because our interests involve the potential use of organometallic dendrimers as catalyst, we used atomic-level computer simulations to investigate the organochromium PBPE dendrimers and the organic PBPE dendrimers for comparison. Our calculations were, however, limited to a maximum of fifth generation size dendrimers because the CPU time scales as N^2.

2. Objectives

We present here the results of our MD simulations for generations 1−5 of the organic PBPE dendrimers and generations 1−5 of the organochromium dendrimers that are the focus of our synthetic work. Each of the generations was simulated for 600 ps and the computations were performed on a Silicon Graphics O2 workstation comprising a R5000 processor and an IBM 43P RS6000 workstation. The 10 simulations took more than a total of 2 CPU months. As far as we are aware, no MD simulations of the family of organometallic PBPE dendrimers have been reported. Furthermore, no detailed calculations on any organometallic dendrimers have been reported to date.

We discuss generalities of the computational methods used in this study in section 3. Several important properties of the macromolecules, namely polymer dimensions, density distributions, monomer density profiles, and SAS, were investigated and are reported in section 4. Here the analysis of the radial density distributions is shown to provide very useful detailed structural information about these macromolecules. In particular, the spatial location of the terminal groups has been determined, and inferences drawn as to the accessibility of the chain ends. We will show that our simulations of organic PBPE dendrimers correlate well with experimentally determined structural features, whereas the organometallic dendrimers we simulated behave differently for dendrimers greater than generation 3. The information obtained from monomer density distributions is compared with the results of the SAS calculations for the organometallic PBPE dendrimers to evaluate the potential applicability of these polymers as catalyst supports.

3. Computational Methodology

We performed all molecular mechanics and dynamics calculations using the program CHARMM.[26] An existing CHARMM-like force field, under development in our laboratory,[27] was modified to model the organometallic dendrimer. All bonds and angles not involving the Cr metal ion were modeled using the usual harmonic potential given by

$$E_x = \Sigma\, k_x\,(x - x_0)^2 \qquad (1)$$

where x is bond length or angle, and x_0 is equilibrium bond length or angle. The $Cr(CO)_3$ group was bonded to the benzyl via a dummy atom located at the center of the benzene ring. We used a scheme similar to that of Doman et al.[28] when treating forces on the dummy atom. By placing the dummy atom at the centroid and "bonding" it to the ring atoms, we ensured that the forces on the dummy atom were equally distributed onto the ring carbons. Furthermore, for the metal-centered torsion angle rotations, we used a Fourier potential truncated at the leading term. The Fourier energy E_F is given by

$$E_F = \Sigma\, k_F\,[1 + \cos(n\phi - \delta)] \qquad (2)$$

where k_F is the torsional force constant, n is the periodicity, ϕ is the angle, and δ is the phase shift. We

Table 1. Parameters for Metal-Centered Torsion Angle Rotations

dihedral angle	k_ϕ	n	phase[a]
CA-DUM-MCR−CM	0.155	6	180.0
CA1-DUM-MCR−CM	0.155	6	180.0
X-MCR−CM-X	0.05	4	0.0

[a] The phase is the minimum geometry of the dihedral.

use a single Fourier angle for the [$Cr(CO)_3Cp$] group with $n = 6$ and $\delta = 180°$. We found in our parametrization procedure that the rotation about the Cr-dummy atom "bond" is principally governed by the nonbonded interactions. A set of relevant Cr parameters related to eq 2 is listed in Table 1. Furthermore, a full account of the performance of the force field is given elsewhere.[29]

3.1. Method for Conformational Analysis of the Repeating Dimer Unit. The central dihedral angle Ψ of the dimer repeat unit shown in Figure 2(b) is the most important when considering the overall dendrimer structure. If this torsion angle is 180°, then the ether linkage will be fully extended, and the resulting dendrimer built with this conformation will have a very open, extended structure. Alternatively, if this dihedral angle is 0°, then the molecule will be folded back on itself, and the resulting dendrimer will be highly condensed. The two remaining dihedrals Φ and Ω, determine the orientation of the aromatic rings. Thus, together, the three dihedral angles define the topology of the entire dendrimer. This is why the main torsion angle Ψ was carefully parametrized and is reported elsewhere with the rest of the force field used in these simulations.[29]

To find the lowest energy conformation of the ether linkage, the energy surface was mapped for a model compound, which we will refer to as the dimer throughout this paper. The dimer, depicted in Figure 2(b), consists of two 3,5-dihydroxybenzyl alcohol monomers connected via an ether linkage, and best represents the interior structure of the dendrimer. Two energy surfaces were calculated, one as a function of the torsion angles Φ, Ψ and the other as a function of the torsion angles Ψ, Ω. These energy surfaces are shown in Figure 3 and discussed in section 4.1.

The energy surface was mapped as a function of the two torsion angles Φ and Ψ, (or Ψ and Ω) by rigidly rotating through all the Φ/Ψ (or Ψ/Ω) combinations through 360° at 30° intervals. At each interval, the lowest energy local minimum was found by stepping through 96 permutations of allowed alcohol group orientations, followed by minimization.

3.2. Protocol for MD Simulations of Dendrimers. The MD simulations were run keeping chemical bonds involving hydrogens fixed via the constraint algorithm SHAKE.[30] The long-range interactions were decreased smoothly to zero between 12 and 14 Å using the CHARMM switching and smoothing functions on an atom-by-atom basis. The equations of motion for the dendrimers were integrated in steps of 1 fs, using a Verlet algorithm.[31]

A rough estimate of the relaxation times of PAMAM dendrimers was reported previously.[20] It was predicted that for later (seventh to ninth) generation PAMAM dendrimers, the relaxation times are in the microsecond regime. This property is strongly related to dendrimer size, thus dendrimers smaller than the sixth generation are expected to exhibit relaxation times around 100 ps.[20] This is a more manageable time frame for atomistic MD simulations. Consequently, the simulation, beyond the initial 15 ps heating stage (100−300 K), was run for 600 ps. During this period, the velocities were periodically rescaled to maintain the correct temperature of 300 K, effectively resulting in a canonical ensemble.

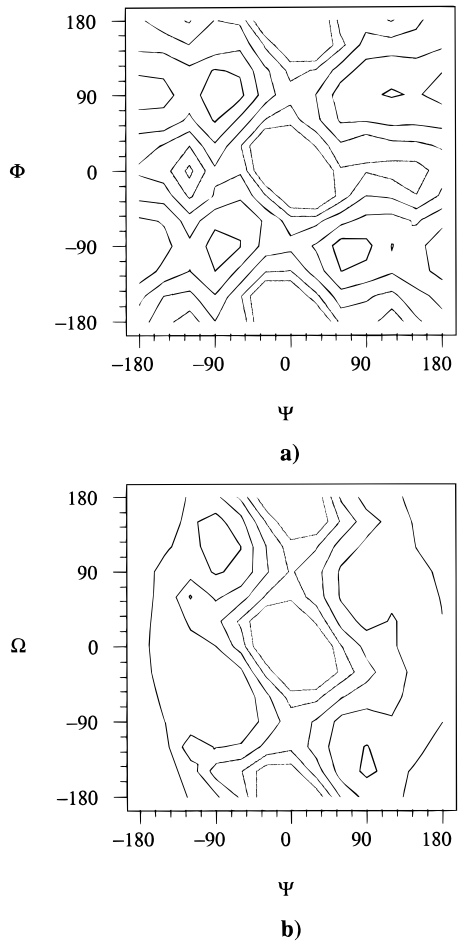

Figure 3. Conformational energy surfaces as a function of the torsional angles joining (Φ, Ψ, and Ω) the monomers (benzyl rings)Ψ−Φ (a) and Ψ−Ω (b). Contours are at 2 kcal·mol^{-1} above the global minimum.

4. Results and Discussion

4.1. Conformational Analyses of the Dendrimer Repeat Unit. From both contour maps (shown in Figure 3), it is clear that the value of the torsion angle Ψ determines the energetic preference of a conformation. There is, in both surfaces, a high-energy region for $\Psi = 0°$, and a low energy trough where $\Psi = 180°$, irrespective of the values of the other torsion angle. The ether link therefore prefers the extended conformation and dendrimers built with this value ($\Psi = 180°$) will have an open, extended structure.

In the Φ/Ψ map, there are low energy troughs where $\Phi = 90°$ and $-90°$ (because of symmetry) which intersect the high-energy region at $\Psi = 0°$. The global minimum of this energy surface is found at (−180°, −90°). The Ψ/Ω map shows a similar surface, with the preferred value of Ω less well defined. Energy troughs are visible around $\Omega = 90°$ and $-90°$, however, the global minimum obtained from this surface is located at (−180°, −150°).

From the two energy surfaces, the lowest energy conformation can be found for the dimer $\Phi = -90°$, $\Psi = -180°$, $\Omega = -150°$. These three torsion angle values,

along with the energy-minimized monomers described earlier, were used to construct the final dendrimers. In this way, the dendrimers should have relatively low strain energy, with fairly open structures and ideal starting conformations for MD simulations. However, from this conformational analysis, note that there are bands of low energy conformations for $\Omega = 90°$ and $-90°$ vs both Φ and Ψ. This low-energy surface in the conformational space of the single dimer will be seen to offer the dendrimer structures a large degree of flexibility that results in folded globular structures after sufficient sampling of phase space. Generations 1−5 of the PBPE organic dendrimers were assembled, along with the corresponding generations of the organochromium dendrimers. Each of the dendrimers was minimized prior to starting the MD simulations.

4.2. Analysis of MD Trajectories. We analyzed the MD trajectories of the PBPE and organochromium PBPE dendrimers for macromolecular dimension, dendrimer geometry, density distributions, monomer density profiles, and SAS.

Dendrimer Dimensions. The time evolutions of the instantaneous radii of gyration (R_G) were calculated for each generation of the organic and organochromium dendrimers and they were found to be qualitatively similar, displaying the same general features. Starting from the initial configuration, the construction of which is described above, the dendrimer was equilibrated. The R_G rapidly decreases over the first 50 ps and stabilizes after this period, to fluctuate around an average value. This indicates that the dendrimer is condensing from the initial extended structure to a far more folded conformation. An illustration of this is given in Figure 4, where the initial structure of a fourth generation organochromium dendrimer and a corresponding structure, which has the lowest energy extracted from the entire dynamics trajectory, are displayed.

It is clear from the folded structure shown in Figure 4 that some of the dimers were able to adopt nonextended conformations which are local minima allowed by the energy troughs displayed in Figure 3. This preference by certain "hinge" dimers away from the global minimum is a consequence of the nonbonded interactions acting as a driving force toward a "condensed structure". The rapid condensation to a globular, folded structure is a result of the simulation being performed in a vacuum. Vacuum simulations are comparable to simulations in a poor solvent. In such a solvent, there are no solute−solvent interactions to compete with the attractive van der Waals and electrostatic solute−solute interactions. Thus the predominant interactions are intramolecular and attractive, so the molecule folds in upon itself. If the dynamics simulations were run in good solvents it is likely that this condensation behavior would be observed to a lesser extent, as was observed in a monomer-level study of dendrimers in solvents of varying quality.[1]

The average radii of gyration were calculated as a function of generation from the time series data discussed above, and are illustrated in Figure 5(a). The initial preequilibration stages of the simulation were excluded from the calculation of the average properties. The average size of the organochromium dendrimers is larger than that for the corresponding organic dendrimers. The average R_G increases not quite linearly with generation, as shown by the data in Figure 5(a). These trends correspond to trends in the hydrodynamic radii

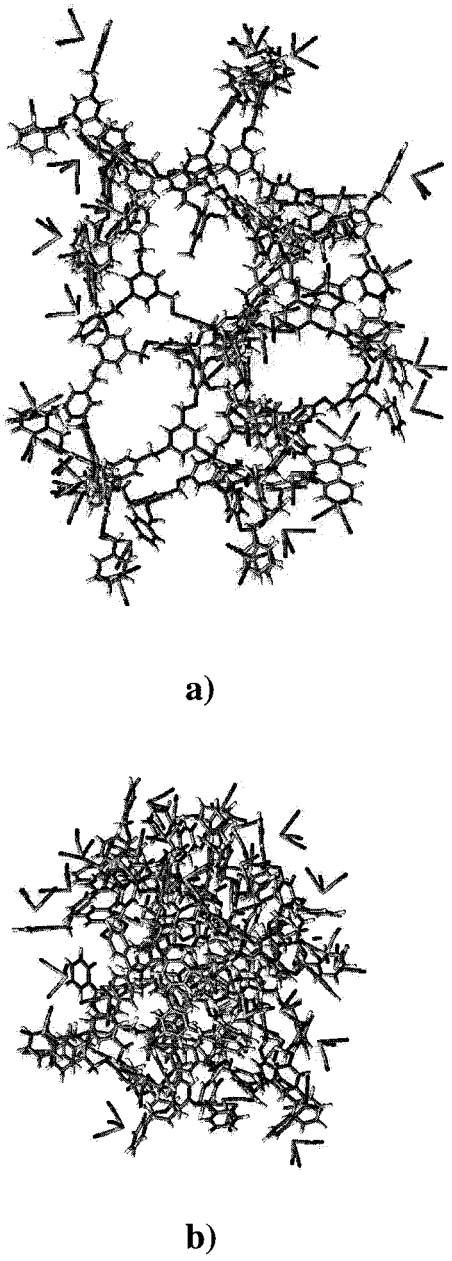

Figure 4. Extended starting structure (a) and the folded low-energy conformation (b) of a fourth generation organochromium dendrimer.

as a function of generation calculated from intrinsic viscosity measurements[32] and with R_G calculations from previous monomer-scale simulations.[1]

In addition to the radius of gyration, the instantaneous root-mean-square (RMS) variation of the dendrimers from their initial structures was calculated. This too provides an indication of whether the system has reached equilibrium. The individual RMS variation time series are qualitatively similar; however, substantially more fluctuation is observed in the later generations. As in the radius of gyration time series, the system equilibrates rapidly within the first 100 ps, after which time it stabilizes and fluctuates around an average value. We observe a discontinuity in the RMS time series of the fourth generation organochromium dendrimer, which appears to be due to one dendron unfolding, while another folds inward to fill the void. The relationship between RMS variation and genera-

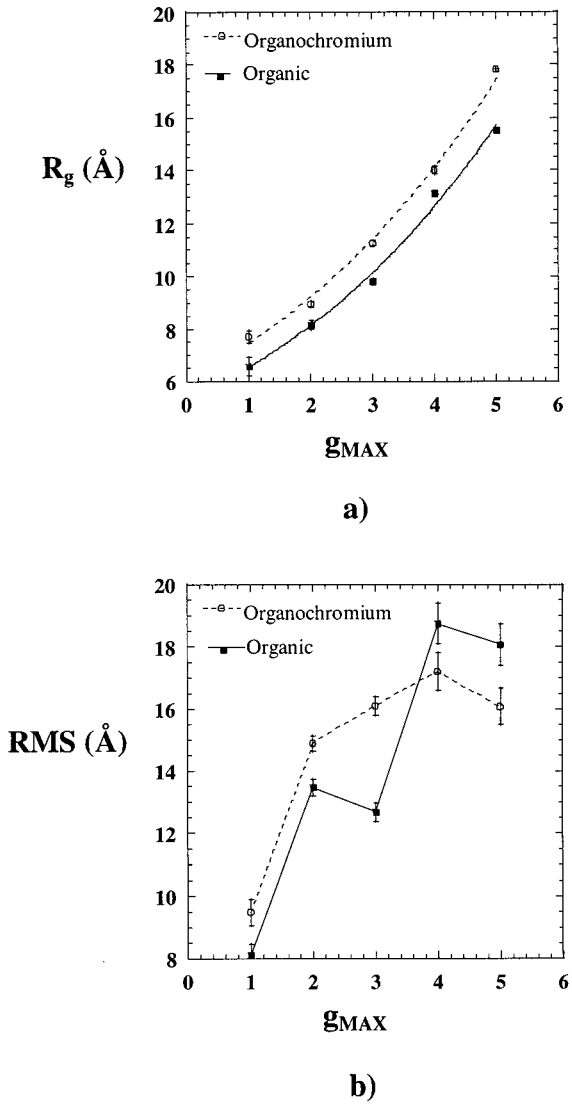

Figure 5. Average radius of gyration vs molecular weight (MW) for the organochromium and organic dendrimer (a). The RMS variation vs generation for the organochromium and organic dendrimer (b)

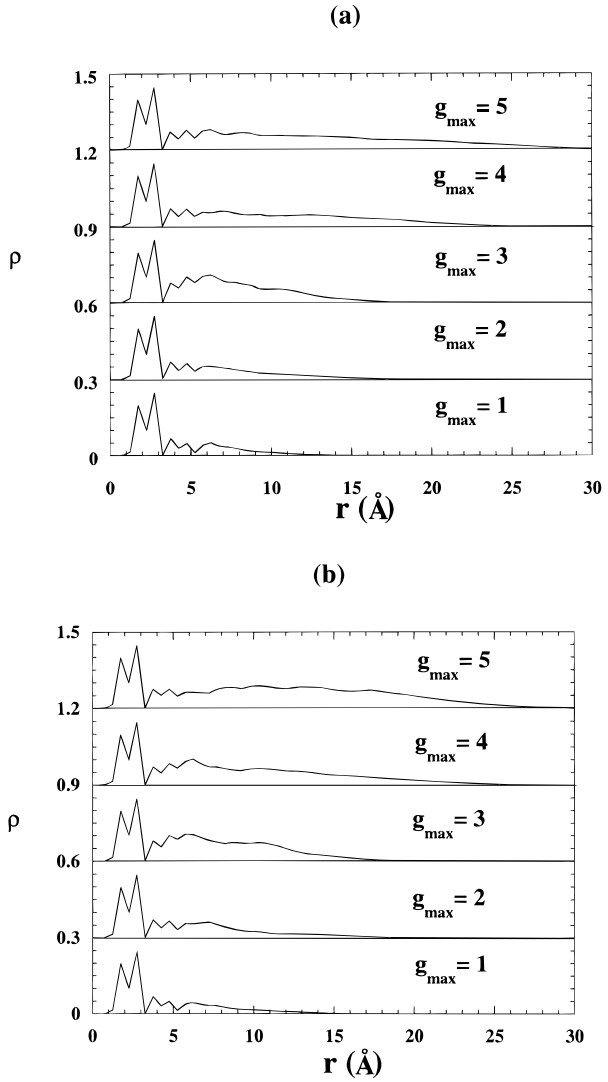

Figure 6. Density profile of the organic (a) and organochromium (b) dendrimer series.

tion, displayed in Figure 5(b), is not as transparent as in the radius of gyration study. The deviation from the mean associated with the RMS variation is larger, because of the increased fluctuation around the average values.

Both the organic and the organochromium dendrimers appear to go through a significant change at the later generations, which could be attributed to a transition from a more open structure to a globular condensed structure, as proposed in other studies.[13,16] This behavior is more noticeable for the organochromium dendrimers, where the RMS variation goes through a maximum at the fourth generation, but is also observed for the organic dendrimers. The RMS variation is less for the organochromium dendrimers smaller than generation 3 compared with the organic dendrimers. However, for generations 4 and 5 there is a greater RMS variation in the organochromium versus the organic dendrimers.

Density Distributions. We calculated the atomic density, as given in eq 3 below, for each dendrimer in an attempt to describe the internal structure of these macromolecules. To this end we determined the number of atoms $N(r)$ within a spherical shell of radius r and thickness δr, averaged over configurations in the range 300−600 ps, and divided by the volume of the shell. The density, $\rho(r)$, is defined below as a function of the number of atoms in a shell.

$$\rho(r) = N(r)/4\pi r^2 \delta r \tag{3}$$

The density profiles of the organic and organochromium dendrimers, illustrated in Figure 6 (a) and (b), respectively, are consistent with the findings of all the previous simulation studies,[1,18−20] and in disagreement with the theoretical model proposed by de Gennes and Hervet. For simplicity, the terminology described in a previous study,[1] will be employed here to differentiate between the generation number of the dendrimer, denoted g_{max} and the individual generations within a dendrimer, denoted g_i.

The profiles of each series have common features. After an initial induction distance, the density of each generation g_{max} is at its highest near the center, and decreases to a minimum at a distance of 3 Å away from the core. Beyond this minimum the density increases away from the center for a period, before tailing off. This is qualitatively consistent with the results of coarse-grained studies except for the induction distance, which was not observed in those calculations.[1,18−21] This

induction distance is due to the inclusion of atomic detail such as the bond lengths of the core part of the molecule. The density profile findings reported here are in good agreement with all of the previous simulation studies.[1,18,19] The region of very high density at the core, which is present in all generations, can be attributed to the atoms belonging to the central core monomer. The remaining density is due to the atoms of the rest of the molecule. As expected for a condensed macromolecule, the density increases and extends further from the core with increasing generation.

A comparison of the density profiles of the organic and organochromium dendrimers highlights a significant difference between the two systems. The peaks resulting from each generation occur at approximately the same radial distance from the core. However, the tail zone, where the density decreases gradually, extends slightly further in the organometallic dendrimers, with the exception of the fifth generation, which extends to the same distance as the fifth generation organic dendrimer. The density is greater in the midrange (5−15 Å) of the third through fifth generation organometallic dendrimers, resulting in regions of almost constant density before sharply tailing off as a result of the finite molecular size. We deduce from this that the monomers of organochromium dendrimers later than generation 3 undergo less backfolding compared with the organic case.

Fractal Geometry. The fractal geometry of these macromolecules can be determined from R_G and $\rho(r)$ calculations. The molecular weight increases exponentially with generation for dendritic molecules. We present a log−log plot of the average radius of gyration as a function of molecular weight (shown in Figure 7 (a)) which removes the inherent quality associated with this special class of branched polymers. The points correspond to the measured averages, whereas the lines are best fits of the form [$R_G = A(\mathrm{MW}t)^x$]. The value of x is 0.31 for the organochromium dendrimers and 0.30 for the organic dendrimers. This corresponds to fractal dimensions of 3.2 and 3.3, respectively. This result is consistent with the calculations of Murat and Grest[1] where the PAMAM-like dendrimers were predicted to have a compact structure.

The results of a further analysis performed to establish the fractal dimensions from the degree of self-similarity of generations 1 ($g_{max} = 1$) through 5 ($g_{max} = 5$) of both the organic and organometallic dendrimer give slightly higher values. Here we first determined the number of atoms *M(R)* as a function of the distance *(R)* from the core center that is defined as

$$M(R) = 4\pi \int_0^R r^2 \rho(r) \mathrm{d}r \qquad (4)$$

Plotting *M(R)* vs *R* for both organic and organochromium dendrimers ($g_{max} = 5$ cases shown in Figure 7 (b)) and fitting the curve to the relation $M(R) = AR^{df}$, we determine the fractal dimensions (d_f). We discarded the tail of the density plot because the integral saturates as a result of the finite size of the dendrimer. The power law fit for the remaining data points curve gives at least a 0.999 correlation. The fifth generation organic and organochromium dendrimers gave best-fit values of $d_f = 2.5$ and $d_f = 2.89$, respectively. These fractal dimensions are in contrast to the values derived from the radius of gyration data and the data of Murat and Grest,[1] but are similar to those calculated by Mansfield[33] for larger dendrimers ($6 \le g_{max} \le 9$). Murat and Grest suggested that the limited self-similarity region in these dendrimers introduced a large error into the data and is partially the reason for the discrepancy. We believe this to be the case here. Nonetheless, despite these differences these values imply that the PBPE dendrimers are highly compact structures.

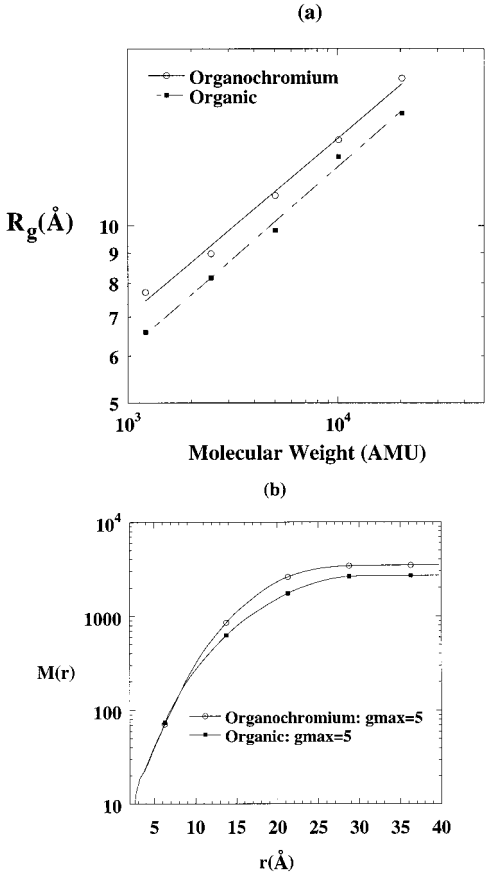

Figure 7. (a) Average radius of gyration vs molecular weight (MW) for $g_{max} = 1-5$ organic and organometallic dendrimers. (b) Number of monomers *M(r)* within a sphere of radius *r* from the center of the organic and organochromium ($g_{max} = 5$) dendrimers.

Monomer Density Profiles. A more telling analysis of the dendrimer internal structure is the distribution of monomers (phenyl groups) as a function of the radial distance from the core. The distributions of the last generation of monomers, which are functionalized by catalysts, are of particular interest to us. We calculated monomer density profiles for each generation (i.e., $g_{max} = 1-5$) of the organic and organochromium dendrimers and the results are displayed in Figures 8 and 9, respectively. The various contributions to the total density $\rho(r)$ from each generation of growth are illustrated for every generation of dendrimer (i.e., $1 \le g_i \le g_{max}$).

These monomer density profiles of the organic dendrimers in Figure 8 (a)−(e) show that the peak due to g_1 is not localized, and in fact splits into several peaks in the later generations. This is mainly a reflection of the random folding displayed by the three wedges. Furthermore, in the early generation dendrimers ($1 \le g_{max} \le 3$) there exists a significant contribution to the total monomer density within the core region from the second and third (g_2 and g_3) generation monomers. The g_2 and g_3 densities extend only slightly further from the

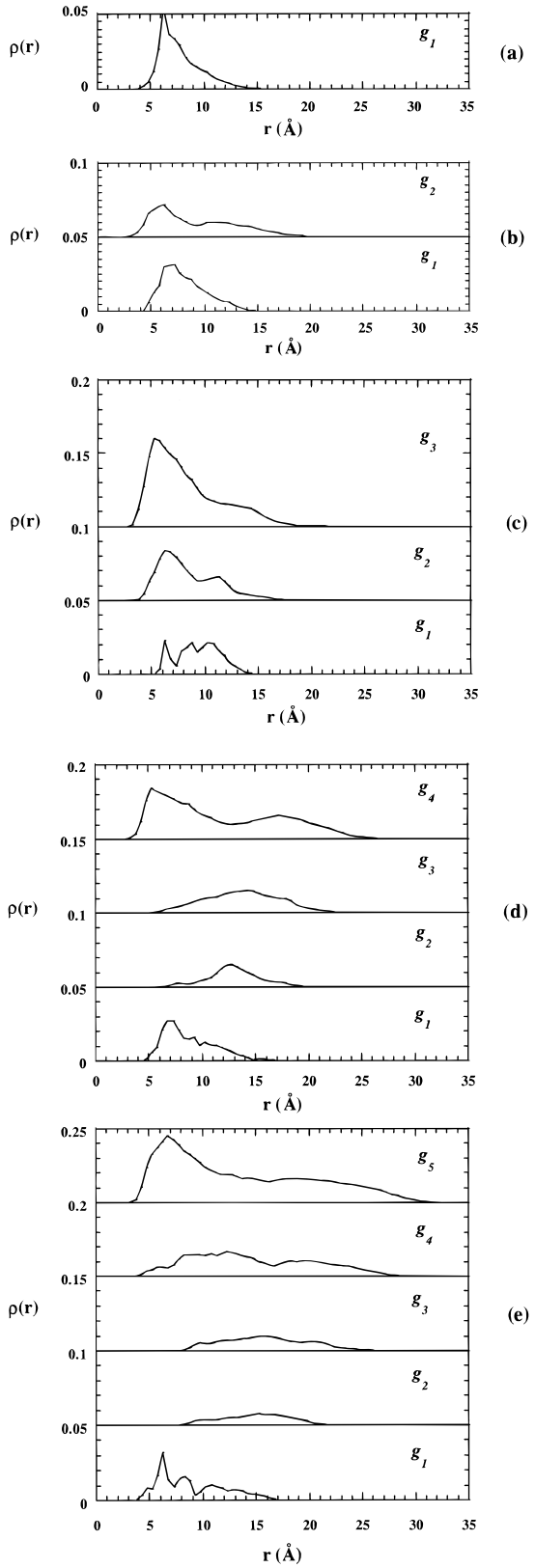

Figure 8. Monomer density profiles for organic dendrimers (a) $g_{max} = 1$, (b) $g_{max} = 2$, (c) $g_{max} = 3$, (d) $g_{max} = 4$, and (e) $g_{max} = 5$.

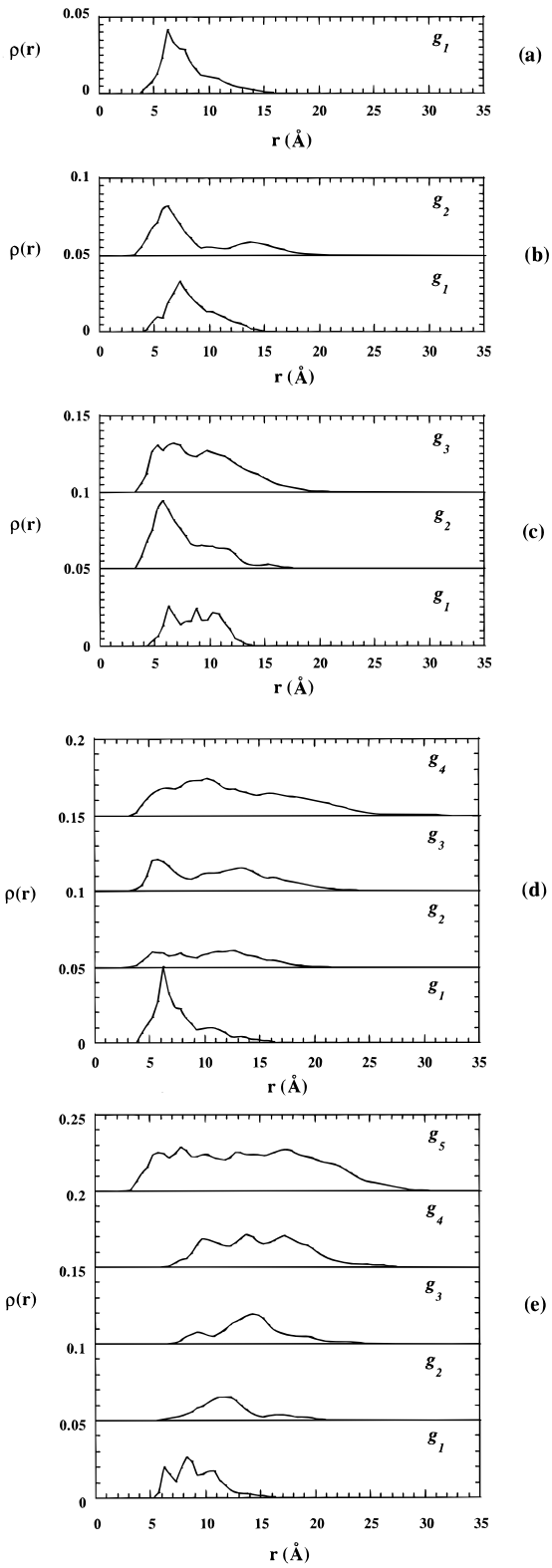

Figure 9. Monomer density profiles for organochromium dendrimers (a) $g_{max} = 1$, (b) $g_{max} = 2$, (c) $g_{max} = 3$, (d) $g_{max} = 4$, and (e) $g_{max} = 5$.

core than does the g_1 density, indicating that the monomers of these generations fold back freely into the center of the dendrimer.

At $g_{max} = 4$, a marked change occurs. The density peaks resulting from the monomers of the early generations are shifted to a larger distance from the core according to generation, so that the peak because of the g_3 is at a further distance than the peak because of the g_2. In addition to this, there is no longer any density because of these generations within the core region. This implies that these monomers have become extended and no longer fold freely. Only the last generation of

monomers is capable of penetrating into the core region of the dendrimer. It is likely that the increased density at the interior as a result of the backward folding of the chain ends hinging about the monomers from g_3 favors the extended conformation of inner monomers. The picture for $g_{max} = 5$ is similar, with the last two generations displaying significant density at the interior, but with only the last generation exhibiting any density within the core region. These results are consistent with the solid-state REDOR experiments performed on organic PBPE dendrimers.[12] The average intramolecular $^{13}C—^{19}F$ distances for generations 3−5 were each approximately 12 Å, which implies an increase in backfolding of the chain ends with increasing generation number, as is the case in our simulations of the organic PBPE dendrimers. Furthermore, our results for these organic PBPE dendrimers compare well with the solution experimental measurements of Hawker et al.[13] Their results for PBPE dendrimers, containing a solvatochromic probe at the core of the molecule, provide evidence for a transition from extended to globular structure.[13] Small changes in the polarity of the environment of this probe cause changes in the UV−vis spectra. This allowed the authors to study the microenvironment of the core as a function of generation. In low-polarity solvents, a significant change in the absorption maximum was observed between generations 3 and 4.[13] This change was correlated to a crossover from an extended to a dense, globular structure.

In all cases, significant overlap between the peaks as a result of each generation is observed. Generally, as the generation of the dendrimers increases from $g_{max} = 1$ to $g_{max} = 5$, the peaks and tail zone of each generation shift to a further distance from the core as a result of all generation monomers becoming extended (with the exception of the outer generations). The terminal monomers are found in all regions of the dendrimer, including the core. These results are qualitatively similar to the previously reported monomer density profiles. However, there are important differences, one being that the monomers are not as localized for small values of g_{max} as found in the previous study;[1] a second reason is that no region of constant density is observed in the density profiles of the generations investigated.

Monomer density profiles for the organochromium system displayed in Figure 9 (a)−(e) exhibit behavior very similar to the organic dendrimers for the early generations $1 \leq g_{max} \leq 3$, with the monomers of the early generations free to fold back and penetrate the core region. However, the profile for $g_{max} = 4$ (Figure 9 (d)) differs from that for the corresponding organic dendrimer (Figure 8(d)). In the organic molecule, the monomers of g_2 and g_3 are extended and so the density peaks resulting from these are localized and shifted away from the core. This behavior is not observed to the same extent in the organometallic dendrimer, because the peaks resulting from g_2 and g_3 are not localized, but are shifted away from the center and dispersed across a larger volume. Furthermore, the last generation of monomers does not undergo sufficient backfolding to enter the core region either, unlike in the organic dendrimer. The chromium carbonyl group makes the ends of the organochromium dendrimers significantly bulkier than the organic end groups. This may inhibit free backfolding as found for the organic PBPE. Consequently, the early generation monomers are not as fully extended in the condensed organochromium dendrimer beyond $g_{max} = 3$. The result is a diminished contribution to the density at the interior from the terminal g_4 monomers in comparison with the organic system.

The density profile for the fifth generation dendrimer (Figure 9(e)), shown above, is mostly similar to the corresponding organic dendrimer. The monomers of the last generation are found in all regions of the dendrimer, including the core, and so the monomers of the early generations become extended. This results in the localization of the density peaks due to g_2 and g_3. Once again the fourth generation monomers are capable of backfolding to a large extent, although they still cannot enter the core region because of molecular crowding. In addition, the density profile of the terminal group g_5 is different for the organochromium case (Figure 9(e)); it makes a lower contribution to the core compared with the organic dendrimer (Figure 8 (e)). In this case the g_5 profile displays a region of almost constant density. As in the previous generation ($g_{max} = 4$) the bulky chromium carbonyl end groups are unable to penetrate the center of the dendrimer.

From density profiles of the organic dendrimers it is clear that the terminal groups are present in the interior of the dendrimer to a significant extent. This indicates that they are mobile and able to penetrate regions of the dendrimer that the other generations cannot. The situation is not the same for the organochromium dendrimers. We observe a break in free penetration of the terminal groups for generations greater than $g_{max} = 3$. Our simulations predict that the physical nature of the end group plays a significant role in the degree to which it is able to backfold. The degree of backfolding at least for organochromium dendrimers appears to decrease with increase in generation number for dendrimers beyond $g_{max} = 3$. This result is in opposition to the results of our own simulations for the organic PBPE dendrimers and the experimental results of Wooley et al.[12]

SAS. Another measure of the accessibility of the chain ends is the calculation of the SAS of these groups. This property is calculated by rolling a sphere of radius P (P = effective radius of solvent) around the van der Waals surface of the molecule. If the SAS of the outer monomers is measured in this way, an indication of their availability can be obtained. There have been SAS calculations on PAMAM and polyether dendrimers with the aim of investigating their internal surface area.[2] Because the chemical availability of the organometallic moiety is of prime interest in this study, the SAS was calculated for the tricarbonylchromium group only.

The starting (fully extended) structures for the MD simulation were used as reference structures. The open, extended conformation of the dendrimer in this state is taken as having 100% SAS. The SASs of these structures were calculated, along with the SASs of the lowest energy configuration of each dendrimer from the dynamics simulation. The SAS of the dendrimer was also calculated as an average over the entire dynamics trajectory. These values are listed in Table 2. From the table it is clear that the SAS decreases with generation number, although all generations possess a significant SAS (>70%), indicating that most of the terminal groups are available for participation in a potential chemical reaction.

It is also clear that the third generation dendrimer has the lowest percentage of SAS. This finding can be

Table 2. The Measured Values of the SAS

generation	initial configuration	average configuration	lowest energy configuration	% SAS (ave/initial)
1	38.39	32.68	33.21	85.13
2	38.39	31.85	32.00	82.96
3	38.42	28.52	27.61	74.23
4	32.45	27.38	26.21	84.37
5	31.84	25.85	25.35	81.19

correlated to the monomer density profile of $g_{max} = 3$, where the g_3 monomers are folded back into the core region to a substantial degree. The fourth and fifth generation organochromium dendrimers would thus be a better choice for catalysis, because they contain relatively large numbers of chain ends, which do not penetrate too deeply into the interior of the dendrimer and also display good solvent accessibility.

5. Conclusions

The de Gennes−Hervet model proposed that the terminal groups are rigid and inflexible, and are located exclusively at the periphery of the molecule.[15] This finding is inconsistent with our simulation results and the results of all of the monomer-level studies.[1,18−21] We observed the effects of molecular crowding where significant chain folding occurs resulting in the branch ends being found in all regions of the dendrimer, as evidenced by the density profiles of these groups. Our conformational analysis on the dimer predicts a definite global minimum with an extended conformation. However, the bands of low-energy conformations for $\Omega = 90°$, $-90°$ and $\Phi = 90°$, $-90°$ in both maps vs Ψ do include several low-energy nonextended conformations. Thus, despite the dimer's conformational preference for an extended structure, when placed in the dendrimer environment the nonbonded monomer−monomer interactions dominate and induce the macromolecule to condense. These low-energy dimer conformations are subsequently found in equilibrated dendrimer structures and facilitate the folding of the macromolecule from an extended to a condensed globular polymer in our vacuum simulations.

The density distributions of all five generations were calculated for both dendritic systems, and the results agree well with the coarse-grained simulation studies. Although the organic PBPE dendrimer correlates well with experiments performed in the solid state[12] and in solution,[13] the simulation results for the organometallic dendrimer deviate from these experimental results. The results of an analysis of monomer distribution within each dendrimer are in general agreement with previous work,[21] but are uniquely applicable to the PBPE system under investigation, because atomic details were taken into consideration in this study. For the first few generations $1 \leq g_{max} \leq 3$, the monomers belonging to generations g_1, g_2, and g_3 seem capable of significant backfolding for both the organic and organochromium dendrimers. For the organic dendrimers $g_{max} = 4$ and 5, significant density because of the outer monomers is found in all regions of the dendrimer, including the core region. This indicates that the chain ends are mobile and are capable of burrowing deep into the molecule. The same is not true for the chromium-carbonyl-loaded chain ends of the organochromium dendrimers. Here the monomers of the terminal generation are less concentrated in the core region compared to the equivalent $g_{max} = 4$ and 5 organic dendrimers. In particular, backfolding in the fifth generation organochromium dendrimer is moderate, giving rise to a region of almost constant density running from the core through most of the dendrimer interior.

Our calculations did not include the effects of the solvent. However, Murat and Grest performed computer simulations to investigate solvent effects on several properties of coarse-grained model dendrimers approximating PAMAM topology. Their simulations revealed that solvent quality had only a small effect on the density distribution, because the radial distribution functions remained essentially the same. The only difference they observed is that as the solvent was varied from good to bad, the height of the constant density region increased, while the width decreased.[1] This indicates that the internal monomers become more condensed in a poor solvent. Radial density profiles of the monomers of each generation are also affected by the solvent quality to a certain degree. The peaks resulting from each generation are shifted to a smaller distance from the core in worse solvents. These results are consistent with another finding by the same authors that the dimensions of the dendrimers shrink as the solvent quality decreases.[1] Moreover, even though we investigated a specific organometallic system via vacuum atomistic computer simulations we believe that these results are relevant to similar organometallic dendrimers. The results presented here are consistent with the monomer-level studies of Murat and Grest for a topologically similar dendrimer system. We are therefore reasonably confident (within the limits of our model) that our structural predictions from vacuum simulations can be generalized to include PBPE dendrimers in a variety of solvents.

The results of the monomer density profile study were compared to those of the SAS calculation. We found that the SAS of the organometallic moiety decreases to a small extent with generation. The third generation dendrimer undergoes significant backfolding of its terminal chromium group and has the lowest percentage of SAS, indicating that this generation of dendrimer would yield the poorest performance-to-cost ratio of the series studied here. On the basis of these results, if we were to recommend a metal carbonyl PBPE dendrimer size for use as a super catalyst, all generations except $g_{max} = 3$ would be ideal. Although the terminal groups are found to some extent in all regions of the dendrimer, the majority of these monomers are still located at the periphery of the molecule, or more precisely, in an SAS for every generation of dendrimer studied here. Therefore, it would appear that even though the study was carried out in comparatively poor solvent conditions, the surface groups of the dendrimers are fairly accessible. If, however, catalytic reactions were to be performed with these dendrimers in a better solvent, it is likely that the reactivity of the system would be enhanced. Consequently, because the all-important terminal catalysts in organometallic PBPE are available to participate in chemical reactions, we expect to access heterogeneous catalytic advantages with an inherently homogeneous setup.

Acknowledgment. This work was support by the Foundation for Research and Development (FRD Pretoria, South Africa) grant number 2037081 to K.J.N. S.J.H. wishes to thank AECI Limited for the 1997 postgraduate student fellowship and Dr. G. Mercier for a helpful dendrimer builder.

References and Notes

(1) Murat, M.; Grest, G. S. *Macromolecules* **1996**, *29*, 1278−1285.
(2) Tomalia, D. A.; Naylor, A. M.; Goddard, W. A. *Angew. Chem., Int. Ed. Engl.* **1990**, *29*, 138−175.
(3) O'Sullivan, D. *Chem. Eng. News* **1993** August 16, 20−23.
(4) Service, R. F. *Science* **1995**, *267*, 458−458.
(5) Tomalia, D. A.; Dvornic, P. R. *Nature* **1994**, *372*, 617−618.
(6) Liao, Y.-H.; Moss, J. R. *Chem. Commun.* **1993**, 1774.
(7) Bardaji, M.; Kustos, M.; Caminade, A.-M.; Majoral, J.-P.; Chaudret, B. *Organometallics* **1997**, *16*, 403−410.
(8) Lobete, F.; Cuadrado, I.; Casado, C. M.; Alonso, B.; Moran, M.; Losada, J. *J. Organomet. Chem.* **1996**, *509*, 109−113.
(9) Hearshaw, M.; Moss, J. R. *J. Chem. Soc. Chem. Commun.* **1998**, in Press.
(10) Hawker, C. J.; Frechet, J. M. J. *J. Am. Chem. Soc.* **1990**, *112*, 7638−7647.
(11) Hearshaw, M.; Hutton, A.; Moss, J. R.; Naidoo, K. J. *Organometallic Dendrimers: Synthesis, Structural Aspects and Applications in Catalysis*; Newkome, G. R., Ed.; JAI Press: Greenwich, 1998; Vol. 4.
(12) Wooley, K. L.; Klug, C. A.; Tasaki, K.; Schaefer, J. *J. Am. Chem. Soc.* **1997**, *119*, 53−58.
(13) Hawker, C. J.; Wooley, K. L.; Frechet, J. M. J. *J. Am. Chem. Soc.* **1993**, *115*, 4375−4376.
(14) Gorman, C.; Hager, M.; Parkhurst, B.; Smith, J. *Macromolecules* **1998**, *31*, 815−822.
(15) De Gennes, P. G.; Herver, J. *J. Phys. Lett.* **1983**, *44*, L351-L360.
(16) Naylor, A. M.; Goddard, W. A. *Polym. Prepr.* **1988**, *29*, 215−216.
(17) Naylor, A. M.; Goddard, W. A.; Keifer, G. E.; Tomalia, D. A. *J. Am. Chem. Soc.* **1989**, *111*, 2339−2341.
(18) Lescanec, R. L.; Muthukumar, M. *Macromolecules* **1990**, *23*, 2280−2288.
(19) Mansfield, M. L.; Klushin, L. I. *J. Phys. Chem.* **1992**, *96*, 3994−3998.
(20) Mansfield, M. L.; Klushin, L. I. *Macromolecules* **1993**, *26*, 4262−4268.
(21) Carl, W. *J. Chem. Soc., Faraday Trans.* **1996**, *92*, 4151−4154.
(22) Smith, J.; Gorman, C. B. *ACS PMSE Proc.* **1998**, *78*, 226−227.
(23) Bhyrappa, P.; Young, J.; Moore, J.; Suslick, K. *J. Mol. Catalysis A* **1996**, *113*, 109−116.
(24) Bhyrappa, P.; Young, J.; Moore, J.; Suslick, K. *J. Am. Chem. Soc.* **1996**, *118*, 5708−5711.
(25) Huck, W.; van Veggel, F.; Reinhoudt, D. *Angew. Chem., Int. Ed. Engl.* **1996**, *35*, 1213−1215.
(26) Brooks, B. R.; Bruccoleri, R. E.; Olafson, B. D.; States, D. J.; Swaminathan, S.; Karplus, M. *J. Comput. Chem.* **1983**, *4*, 187−217.
(27) Naidoo, K. J.; Ueda, K. Unpublished work, 1998.
(28) Doman, T. N.; Landis, C. R.; Bosnich, B. *J. Am. Chem. Soc.* **1992**, *114*, 7264−7272.
(29) Naidoo, K. J.; Hughes, S. J.; Moss, J. R. submitted for publication, *J. Organomet. Chem.*, 1998.
(30) Ryckaert, J. P.; Cicotti, G.; Berendsen, H. J. C. *J. Comput. Phys.* **1977**, *23*, 327−341.
(31) Verlet, L. *Phys. Rev.* **1967**, *159*, 98−103.
(32) Mourey, T. H.; Turner, S. R.; Rubenstein, M.; Frechet, J. M. J.; Hawker, C. J.; Wooley, K. L. *Macromolecules* **1992**, *25*, 2401−2406.
(33) Mansfield, M. L. *Polymer* **1994**, *35*, 1827−1830.

MA981135G